Thouless Pumps and Bulk-Boundary Correspondence in Higher-Order Symmetry-Protected Topological Phases

Julian F. Wienand,[1,2,3,*] Friederike Horn,[1] Monika Aidelsburger,[1,2] Julian Bibo,[2,4] and Fabian Grusdt[1,2]
[1]Department of Physics and Arnold Sommerfeld Center for Theoretical Physics (ASC), Ludwig-Maximilians-Universität München, Theresienstr. 37, D-80333 Munich, Germany
[2]Munich Center for Quantum Science and Technology (MCQST), Schellingstr. 4, D-80333 Munich, Germany
[3]Max-Planck-Institut für Quantenoptik, Hans-Kopfermann-Strasse 1, D-85748 Garching, Germany
[4]Department of Physics, T42, Technical University of Munich, D-85748 Garching, Germany

(Received 18 November 2021; revised 20 February 2022; accepted 5 April 2022; published 17 June 2022)

The bulk-boundary correspondence relates quantized edge states to bulk topological invariants in topological phases of matter. In one-dimensional symmetry-protected topological systems, quantized topological Thouless pumps directly reveal this principle and provide a sound mathematical foundation. Symmetry-protected higher-order topological phases of matter (HOSPTs) also feature a bulk-boundary correspondence, but its connection to quantized charge transport remains elusive. Here, we show that quantized Thouless pumps connecting C_4-symmetric HOSPTs can be described by a tuple of four Chern numbers that measure quantized bulk charge transport in a direction-dependent fashion. Moreover, this tuple of Chern numbers allows to predict the sign and value of fractional corner charges in the HOSPTs. We show that the topologically nontrivial phase can be characterized by both quadrupole and dipole configurations, shedding new light on current debates about the multipole nature of the HOSPT bulk. By employing corner-periodic boundary conditions, we generalize Restas's theory to HOSPTs. Our approach provides a simple framework for understanding topological invariants of general HOSPTs and paves the way for an in-depth description of future dynamical experiments.

DOI: 10.1103/PhysRevLett.128.246602

Introduction.—Protected edge states are a signature phenomenon in (many-body) quantum systems with nontrivial topology. In one dimension (1D), such accumulation of charge at the boundary can be understood as the consequence of polarization in the bulk. As discovered by King-Smith and Vanderbilt [1], the polarization is a manifestation of the Zak (Berry) phase of the underlying Bloch bands [2,3]. For interacting many-body systems with periodic boundaries this result was later generalized by Resta, who related polarization to the many-body position operator in 1D [4]. The underlying intuition is that building up polarization in the bulk or charge at the boundary requires quantized charge transport as described by topological Thouless pumps [5,6].

With the recent discovery of higher-order topological insulators [7,8], efforts were made to generalize these concepts to describe electrical multipole moments [7–14] and higher-order Thouless pumps [8,9,14–16]. A n-dimensional bulk with topology of order m can exhibit $(n-m)$-dimensional corner or hinge states, when open boundary conditions (OBC) are applied. Such systems have been realized in solids and classical metamaterials [15,17–26]. Higher-order boundary states are anticipated to have versatile applications in electronics and photonics [27], e.g., for topological nanolasers [28,29].

Higher-order topological invariants have been proposed for both band insulators in a single-particle picture (higher-order topological insulators) and interacting quantum many-body systems (symmetry-protected higher-order topological phases of matter, or HOSPTs) protected by crystalline symmetries [8,9,13,14,16,30–37]. Yet, there is an ongoing debate on which of the proposed quantities constitute true bulk invariants and how exactly the multipole polarization can be calculated in extended systems with periodic boundary conditions [11,13]. For instance, recent works [9,13] proposed to extend the work of Resta, which connects the polarization to the Zak (Berry) phase [4], by defining a many-body quadrupole operator. However, these approaches have sparked controversy [11].

In this Letter, we provide a theoretical framework for understanding bulk polarization in HOSPTs. By introducing corner-periodic boundary conditions (CPBC) we extend Resta's argument [4] to higher-order systems. This allows us to describe charge transport between corners

during Thouless pumping cycles in a direction-dependent fashion. Moreover, charge flow can be precisely tracked and an intuitive picture of bulk polarization in HOSPTs emerges.

Our results show that quantized Thouless pumps connecting topologically distinct C_4-symmetric HOSPTs can be characterized by a tuple of four Chern numbers. The underlying Zak (Berry) phases are quantized in the $C_4 \times \mathbb{Z}_2$-symmetric HOSPTs and serve as topological invariants of the latter. The invariants we define are similar to those introduced by Araki *et al.* [32], but without the necessity to introduce magnetic flux in the bulk—hence they yield a definite value for *any* gapped phase in the thermodynamic limit. Our approach allows to directly relate the quantized corner charge in a HOSPT [10,12,38] to the Zak (Berry) phase, giving new physical meaning to the latter.

For concreteness, we discuss interacting bosonic $C_4(\times\mathbb{Z}_2)$-symmetric HOSPTs. For these systems, we propose higher-order Thouless pumps that are in reach of current experiments with ultracold atoms and classical metamaterials [15,39–42]. We show that different types of pumps can create nontrivial HOSPTs in a quadrupole configuration (with vanishing dipole) and a dipole configuration (with vanishing quadrupole); see Fig. 1.

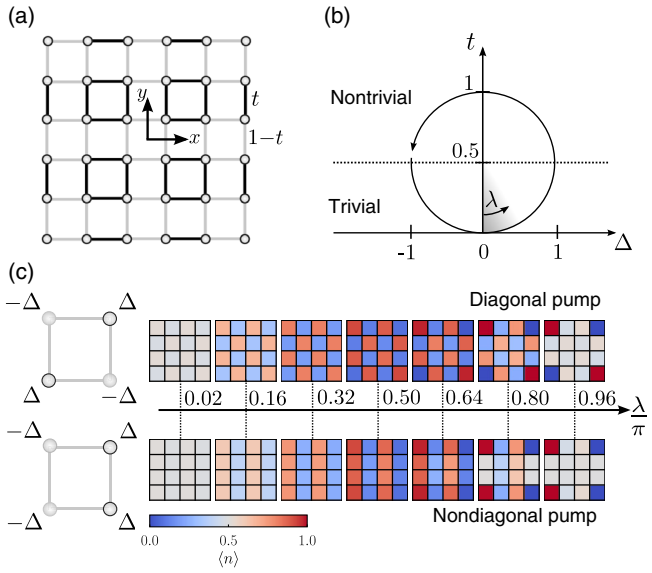

FIG. 1. Thouless pumps in the 2D SL-BHM. (a) Interacting bosons on a square lattice with staggered tunneling (strengths t and $1-t$, respectively) and OBC. (b) Thouless pump, parametrized by $\lambda \in [0, 2\pi)$, as defined in the text, with Δ controlling additional on-site potentials shown in (c). (c) Density evolution during a diagonal (upper panel) and a nondiagonal (lower panel) half-Thouless pump, ending in a quadrupole and a dipole configuration, respectively. On the left the corresponding arrangements of the additional on-site potentials are sketched. For creating a diagonal Thouless pump, in each plaquette shifts of equal sign are added on diagonally opposite sites. For creating a nondiagonal Thouless pump, shifts of the same sign are added on the same side.

Model.—As a hallmark model exhibiting a higher-order symmetry-protected phase, we study the 2D superlattice-Bose-Hubbard model (SL-BHM) [33,38,43], which can be experimentally realized using ultracold atoms [44–47]. On a square lattice with OBC it is defined by the Hamiltonian

$$\hat{H}^{\mathrm{OBC}} = -\left[\sum_{x=-D}^{D-1}\sum_{y=-D}^{D}\left(t(x)\hat{a}^{\dagger}_{x,y}\hat{a}_{x+1,y} + \mathrm{H.c.}\right) + x \leftrightarrow y\right] + \frac{U}{2}\sum_{x,y=-D}^{D}\hat{n}_{x,y}(\hat{n}_{x,y}-1), \tag{1}$$

where $D = (L-1)/2$, $\hat{a}^{\dagger}_{x,y}(\hat{a}_{x,y})$ is the creation (annihilation) operator at site (x, y), $\hat{n}_{x,y} = \hat{a}^{\dagger}_{x,y}\hat{a}_{x,y}$ is the particle number operator, and U is the on-site interaction energy; see Fig. 1(a). The origin (0,0) is the C_4-symmetry center and for $U \to \infty$ the model has an additional $\mathbb{Z}_2$ symmetry, $\hat{a}^{\dagger}_{x,y} \leftrightarrow \hat{a}_{x,y}$. The hopping amplitudes $t(\zeta), \zeta \in \{x, y\}$ are staggered:

$$t(\zeta) = \begin{cases} 1-t & \text{for } \zeta \in \{-D, -D+2, \ldots, D-1\} \\ t & \text{for } \zeta \in \{-D+1, -D+3, \ldots, D-2\}, \end{cases} \tag{2}$$

with $t \in [0, 1]$ controlling the transition from the trivial ($t = 0$) to the topological ($t = 1$) phase [38]. In the following, we propose two types of Thouless pumps in this model.

Thouless pumping cycle.—A Thouless pump is the cyclic adiabatic variation of an external parameter. It leads to quantized charge transport that characterizes the topology of the bulk [5,48]. For the 2D SL-BHM, our full pumping cycle consists of a closed trajectory in a $\Delta - t$ parameter space. It crosses two C_4-symmetric points and avoids closing the bulk gap; see Fig. 1(b). Here, Δ controls the strength of additional on-site potentials whose arrangement dictates the direction of the charge transport. We will show two types of Thouless pumps that transport charge diagonally (diagonal pump) or horizontally (nondiagonal pump). For the former, each plaquette has on-site potentials in a cross-diagonal arrangement (Fig. 1(c), top left); for the latter, each plaquette has on-site potentials with equal sign on the same side (Fig. 1(c), bottom left). The total Hamiltonians then read as follows:

$$\hat{H}^{\mathrm{diag}} = \hat{H}^{\mathrm{OBC}} + \Delta\sum_{x,y=-D}^{D}\hat{n}_{x,y}(-1)^{(x+D)+(y+D)}$$
$$\hat{H}^{\mathrm{nondiag}} = \hat{H}^{\mathrm{OBC}} - \Delta\sum_{x,y=-D}^{D}\hat{n}_{x,y}(-1)^{(x+D)}. \tag{3}$$

The pump cycle is parametrized by $\lambda \in [0, 2\pi)$, with $t(\lambda) = [1 + \cos(\lambda)]/2$ and $\Delta(\lambda) = \sin(\lambda)$, as illustrated in Fig. 1(b). It breaks the C_4 symmetry, except for $\lambda \in \pi\mathbb{Z}$.

In Fig. 1(c), we show the density evolution of the diagonal (upper panel) and nondiagonal (lower panel) pumps with OBC and at half-filling ($N = L^2/2$). We use exact diagonalization for $L = 4$ and assume hard-core bosons, i.e., $U \to \infty$. At the beginning of the pump, charge accumulates at the sites that are subject to negative energy shifts $-\Delta$. Then, once $\lambda = \pi/2$ is passed and $|\Delta|$ decreases, the density evens out in the bulk and along the edges. At the corners, however, the average density increases further up to 1 or down to 0, respectively, until $\lambda = \pi$. This yields four corner-localized fractional charges, two with charge $-1/2$ and two with charge $+1/2$. The arrangement of these corner charges at $\lambda = \pi$ corresponds either to a quadrupole (diagonal pump) or a dipole (nondiagonal pump) configuration.

Higher-order Zak phase and bulk-boundary correspondence in HOSPTs.—Next, we develop a theoretical framework relating the fractional corner charges of the HOSPTs at $\lambda = \pi\mathbb{Z}$ to bulk properties. By introducing CPBC, we define a tuple of Zak (Berry) phases that act as topological invariants for HOSPTs. In addition, each Zak (Berry) phase will be associated with a certain direction, such that its change can be connected to a current operator pointing along that direction.

To achieve CPBC, as illustrated in Fig. 2(a), we add corner-connecting links to the Hamiltonian in Eq. (1):

$$\hat{H}^C = -t(\hat{a}^\dagger_{c_1}\hat{a}_{c_2} + \hat{a}^\dagger_{c_2}\hat{a}_{c_3} + \hat{a}^\dagger_{c_3}\hat{a}_{c_4} + \hat{a}^\dagger_{c_4}\hat{a}_{c_1}), \quad (4)$$

where c_i denotes the coordinates of the ith corner, i.e., $c_1 = (-D, D)$, $c_2 = (-D, -D)$, $c_3 = (D, -D)$, and $c_4 = (D, D)$ with $D = L/2 - 1/2$. The total Hamiltonian with CPBC then reads $\hat{H}^{\mathrm{CPBC}} = \hat{H}^{\mathrm{OBC}} + \hat{H}^C$. With CPBC applied, the four corner sites form one additional plaquette.

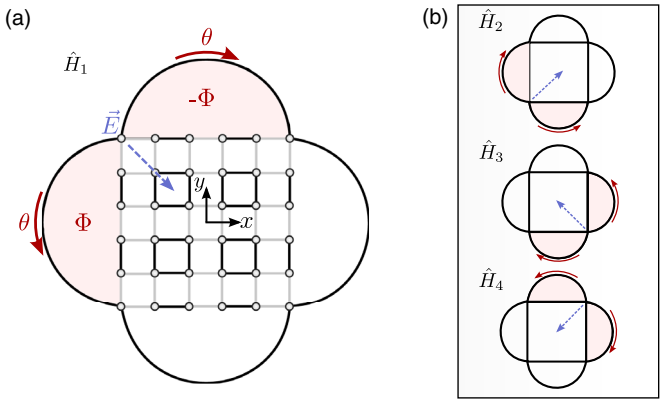

FIG. 2. Direction-dependent sensing of charge flow. Model with CPBC. We propose four gauge choices $\hat{U}_1$ (a), $\hat{U}_2$, $\hat{U}_3$, and $\hat{U}_4$ (b) that are connected by C_4 symmetry, Eq. (5). The Zak (Berry) phases defined on these choices act as sensors of charge flow. They are only sensitive in the direction of the electric field (blue) that is induced when the flux in the outer supercells becomes time-dependent.

They also give rise to four supercells outside the bulk, delimited by the edge of $\hat{H}^{\mathrm{OBC}}$ and one of the corner-connecting links; see Fig. 2(a).

We start by extending the definition of the (many-body) Zak (Berry) phase to higher-order systems. To this end, magnetic flux Φ is adiabatically inserted in the two supercells meeting at corner i. This process is associated with an induced electric field pointing along a diagonal [49] (see Fig. 2) and can be formally described by gauge transformations $\hat{U}_i$, $i \in \{1, 2, 3, 4\}$, which we apply *only* to the corner parts of the Hamiltonian:

$$\hat{H}^C_i(\theta) = \hat{U}^\dagger_i(\theta)\hat{H}^C\hat{U}_i(\theta), \quad (5)$$

with $\hat{U}_i(\theta) = e^{i\hat{X}_i(\theta)}$ and $\hat{X}_i(\theta) = \theta\hat{n}_{c_i}$. Here, $\hat{n}_{c_i}$ is the particle number operator at the ith corner.

The four gauge transformations $\hat{U}_i$ with $i \in \{1, 2, 3, 4\}$ are related to each other through C_4 symmetry, i.e., $C_4^{-1}\hat{U}_i(\theta)C_4 = \hat{U}_{i+1}(\theta)$. The resulting Hamiltonians, $\hat{H}_i(\theta) = \hat{H}^C_i(\theta) + \hat{H}^{\mathrm{OBC}}$, are sketched in Fig. 2: Each gauge transformation adds a phase θ to a pair of corner-connecting links. As desired, the supercells outside the bulk are pierced by a flux $\Phi = \theta$.

Next, separately for each gauge choice $\hat{U}_i$, we define a higher-order Zak (Berry) phase γ_i as the geometric phase picked up by the ground state wave function $|\psi_i(\theta)\rangle$ of $\hat{H}_i(\theta)$ when changing θ from 0 to 2π [2,53]:

$$\gamma_i = \oint_0^{2\pi} d\boldsymbol{\theta}\langle\psi_i(\theta)|i\partial_\theta|\psi_i(\theta)\rangle. \quad (6)$$

We note that, like the 1D Zak phase [2], the higher-order version γ_i explicitly depends on our choice of gauge for inserting 2π flux through the supercells, while the difference $\Delta\gamma_i$ is gauge-invariant.

As a direct consequence of $\mathbb{Z}_2$ symmetry in the case of hardcore bosons, the higher-order Zak (Berry) phase is $\mathbb{Z}_2$-quantized,

$$\gamma_i \in \pi\mathbb{Z} \quad (7)$$

(see the Supplemental Material [49] for an explicit proof).

The higher-order Zak (Berry) phases we introduce are related to the C_4-symmetry-protected geometric phases proposed by Araki *et al.* [32,49]. However, in contrast to the construction in [32], our bulk Hamiltonian $\hat{H}^{\mathrm{OBC}}$ remains independent of θ and our gauge choice creates a twist of the Hamiltonian $\hat{H}_i(\theta)$ *without* introducing flux in the bulk. Hence, the gap remains open during flux insertion in the thermodynamic limit [49], rendering Eq. (6) a well-defined topological invariant. Extending Araki's scheme by introducing their fluxes through our corner-periodic links yields a robust $\mathbb{Z}_4$-quantized invariant protected by C_4 symmetry.

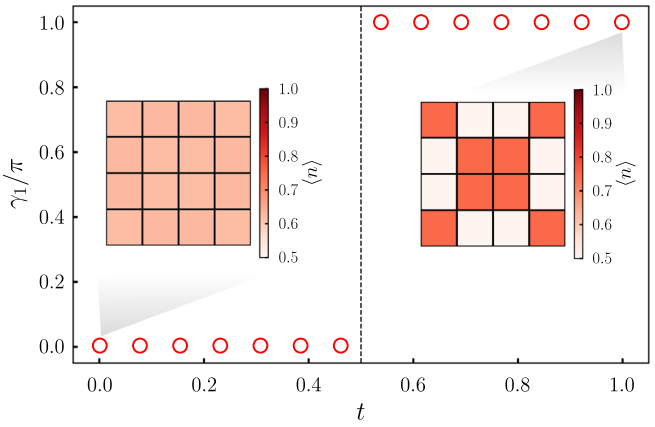

FIG. 3. Quantized higher-order Zak (Berry) phase. We show γ_1 as a function of the tunneling parameter t at half-filling ($N = L^2/2$) and with CPBC for $L = 4$. The insets show the density expectation values of a 4×4 system at filling $N = L^2/2 + 2$. Even though the nontrivial phase ($t > 0.5$) does not exhibit any corner states due to CPBC, the two extra particles above half-filling lead to an occupation imbalance between edge doublets and bulk plaquettes that is unique to the nontrivial phase.

Figure 3 depicts γ_1 as a function of the tunneling parameter t in the SL-BHM at $C_4 \times \mathbb{Z}_2$-symmetric points (the plots for $\gamma_{2,3,4}$ look identical). The wave functions in Eq. (6) were calculated in a small system ($L = 4$) with CPBC. The Zak (Berry) phase is quantized, as predicted, and jumps from 0 (trivial phase) to π (nontrivial phase). With CPBC applied, the nontrivial phase is characterized by a density imbalance between bulk and edge doublets.

Finally, we relate the higher-order Zak (Berry) phase to charge transport and derive a bulk-boundary correspondence for HOSPTs. This is achieved by extending Resta's argument to higher-order systems and introducing a many-body position operator in the bulk (see the Supplemental Material [49], Sec. II for details). A key step in this process is to note that the adiabatic flux insertion in Eq. (5) can be directly related to the current passing diagonally through a corner, $\hat{J}_i = \partial_\theta \hat{H}_i(\theta)|_{\theta=0}$ for $i = 1, \ldots, 4$. Integrating up these currents along an adiabatic path connecting two HOSPTs (e.g., along a half-Thouless pump cycle) yields a total change of the corner charge Δq_{c_i} in corner i, and we can show (Supplemental Material [49], Sec. II F) that

$$\Delta q_{c_i} = -\frac{\Delta\gamma_i}{2\pi}, \tag{8}$$

that is, the fully gauge invariant difference $\Delta\gamma_i$ of the higher-order Zak (Berry) phases in two HOSPTs is directly related to the difference of their corner charges. Since we showed that γ_i is quantized by $C_4 \times \mathbb{Z}_2$ symmetry, it follows that the corner charge Δq_{c_i} is also quantized and represents an intrinsic topological invariant distinguishing HOSPTs.

Chern numbers of higher-order Thouless pumps.—We can now apply the higher-order Zak (Berry) phase defined in Eq. (6) to track the charge flow during the Thouless pumps introduced in Fig. 1. The total amount of charge $\Delta Q_{c_i} = \oint dq_{c_i}$ transported during one full pumping cycle, or equivalently, the amount of charge piling up at the corners as corner states with OBC, can be measured by four Chern numbers $\mathcal{C}_i$ with $i \in \{1, 2, 3, 4\}$. Using our main result from Eq. (8), the latter are obtained as winding numbers of the higher-order Zak (Berry) phase (Note that in the numerical calculations we defined the Berry Phase positively, such that the minus sign cancels.),

$$\mathcal{C}_i = \oint_0^{2\pi} \frac{d\lambda}{2\pi} \partial_\lambda \gamma_i(\lambda) = \sum_n \left[\frac{\gamma_i(\lambda_{n+1})}{2\pi} - \frac{\gamma_i(\lambda_n)}{2\pi} \right]. \tag{9}$$

The second expression is a discretized version, with a sufficiently large number of discrete points $\lambda_n \in [0, 2\pi)$. Our conventions are such that a negative (positive) Chern number $\mathcal{C}_i$ indicates a particle current from the center toward the corner c_i (from the corner c_i toward the center); see the Supplemental Material [49], Sec. II F.

Since the Zak (Berry) phase is defined mod 2π, it follows directly from Eq. (9) that the Chern numbers, $\mathcal{C}_i$, and the associated bulk charge transport along the corresponding diagonal $\Delta Q_{c_i} = -\mathcal{C}_i$, are integer quantized. Note that this remains true even at finite U where $\mathbb{Z}_2$ symmetry is broken. Moreover, by C_4 symmetry, half-Thouless pumps connecting HOSPTs lead to a change of the corner charge $\Delta q_{c_i} = -\mathcal{C}_i/2$ given by half the Chern number. The sum rule $\sum_{i=1}^4 \mathcal{C}_i = 0$ guarantees net charge conservation.

Now we calculate the Chern numbers characterizing the higher-order Thouless pumps introduced earlier for the SL-BHM. Figures 4(b) and 4(d) show the evolution of the four higher-order Zak (Berry) phases as a function of the pump parameter λ. The Chern numbers $\mathcal{C}_i$ are extracted from the windings of γ_i and read $\mathcal{C}^{\text{diag.}} = (-1, 1, -1, 1)$ for the diagonal and $\mathcal{C}^{\text{nondiag.}} = (-1, -1, +1, +1)$ for the nondiagonal pump. The resulting overall charge flow is sketched in Figs. 4(a) and 4(c) for both pumps. The result is consistent with the density evolution we find in Fig. 1 for a system with OBC. There, the half-charged particle (hole) corner states emerge where the associated Chern number is negative (positive)—in accordance with our result $\Delta q_{c_i} = -\mathcal{C}_i/2$.

Our example shows that the tuple of Chern numbers $\mathcal{C}_i$ can describe Thouless pumps building up both a dipole and a quadrupole moment. This sheds light on previously reported difficulties with defining a pure quadrupole operator in systems without dipole conservation [11]. Our case study also demonstrates that three Chern numbers need to be known to distinguish diagonal from nondiagonal pumps.

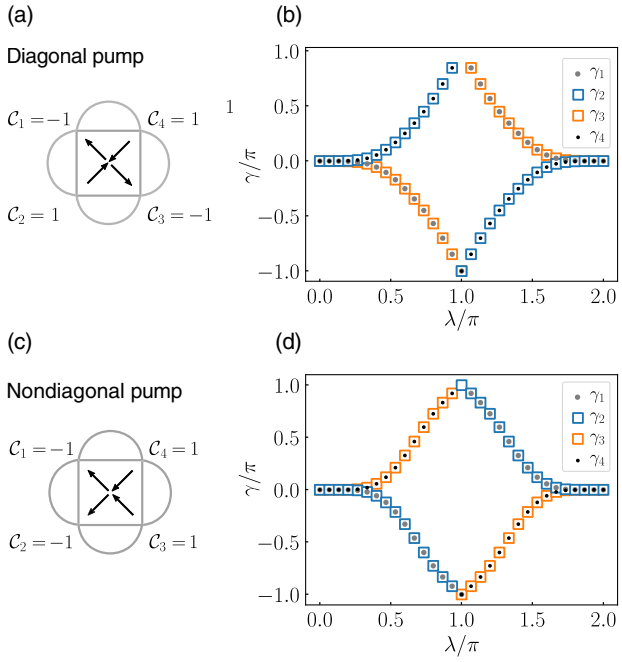

FIG. 4. Chern number tuples for diagonal and nondiagonal Thouless pumps. (b),(d) Evolution of the higher-order Zak (Berry) phases γ_i along the full nondiagonal (lower panel) and diagonal (upper panel) Thouless pumps in the SL-BHM, as defined below Eq. (3). (a),(c) Each Chern number $\mathcal{C}_i$ is associated with the current operator $\hat{J}_i$ defined through the gauge transformation $\hat{U}_i$. A negative (positive) value indicates charge flow to (away from) the corner c_i.

Summary and outlook.—In conclusion, we have investigated quantized charge transport in higher-order topological systems and provided a description of higher-order Thouless pumps. In doing so, we introduced the higher-order Zak (Berry) phase as a new topological invariant of HOSPTs that enters in the bulk-boundary correspondence. We have found a way to extend Resta's earlier work [4] to HOSPTs and relate the many-body Zak (Berry) phase to charge transport in the bulk. For a concrete system with $C_4(\times\mathbb{Z}_2)$ invariance, we demonstrated that a tuple of four Chern numbers characterizes its HOSPTs and can be used to track the emergence of dipoles and quadrupoles in the system's bulk during an experimentally accessible higher-order Thouless pump.

Our approach can straightforwardly be applied to other discrete symmetries, geometries, fillings, or settings without translational symmetry in the bulk. We leave detailed analysis of such cases to future work. Particularly interesting directions include the SL-BHM at quarter filling or quasicrystals constituting HOSPTs.

We thank Frank Pollmann, Izabella Lovas, Christian Schweizer and Cesar Cabrera for insightful discussions. J. F. W. acknowledges support from the German Academic Scholarship Foundation and the Marianne-Plehn-Program. J. B. acknowledges support from the European Research Council (ERC) under the European Union's Horizon 2020 research and innovation program (Grant agreement No. 771537). We acknowledge funding by the Deutsche Forschungsgemeinschaft (DFG, German Research Foundation) via Research Unit FOR 2414 under project no. 277974659, and under Germany's Excellence Strategy—EXC-2111–390814868.

*j.wienand@lmu.de

[1] R. D. King-Smith and D. Vanderbilt, Phys. Rev. B **47**, 1651 (1993).
[2] J. Zak, Phys. Rev. Lett. **62**, 2747 (1989).
[3] M. Atala, M. Aidelsburger, J. T. Barreiro, D. Abanin, T. Kitagawa, E. Demler, and I. Bloch, Nat. Phys. **9**, 795 (2013).
[4] R. Resta, Phys. Rev. Lett. **80**, 1800 (1998).
[5] D. J. Thouless, Phys. Rev. B **27**, 6083 (1983).
[6] Q. Niu and D. J. Thouless, J. Phys. A **17**, 2453 (1984).
[7] W. A. Benalcazar, B. A. Bernevig, and T. L. Hughes, Science **357**, 61 (2017).
[8] W. A. Benalcazar, B. A. Bernevig, and T. L. Hughes, Phys. Rev. B **96**, 245115 (2017).
[9] B. Kang, K. Shiozaki, and G. Y. Cho, Phys. Rev. B **100**, 245134 (2019).
[10] H. Watanabe and S. Ono, Phys. Rev. B **102**, 165120 (2020).
[11] S. Ono, L. Trifunovic, and H. Watanabe, Phys. Rev. B **100**, 245133 (2019).
[12] S. Ren, I. Souza, and D. Vanderbilt, Phys. Rev. B **103**, 035147 (2021).
[13] W. A. Wheeler, L. K. Wagner, and T. L. Hughes, Phys. Rev. B **100**, 245135 (2019).
[14] B. Kang, W. Lee, and G. Y. Cho, Phys. Rev. Lett. **126**, 016402 (2021).
[15] W. A. Benalcazar, J. Noh, M. Wang, S. Huang, K. P. Chen, and M. C. Rechtsman, arXiv:2006.13242.
[16] I. Petrides and O. Zilberberg, Phys. Rev. Research **2**, 022049 (2020).
[17] R. Noguchi *et al.*, Nat. Mater. **20**, 473 (2021).
[18] C. W. Peterson, W. A. Benalcazar, T. L. Hughes, and G. Bahl, Nature (London) **555**, 346 (2018).
[19] S. Imhof, C. Berger, F. Bayer, J. Brehm, L. W. Molenkamp, T. Kiessling, F. Schindler, C. H. Lee, M. Greiter, T. Neupert, and R. Thomale, Nat. Phys. **14**, 925 (2018).
[20] M. Serra-Garcia, V. Peri, R. Süsstrunk, O. R. Bilal, T. Larsen, L. G. Villanueva, and S. D. Huber, Nature (London) **555**, 342 (2018).
[21] J. Bao, D. Zou, W. Zhang, W. He, H. Sun, and X. Zhang, Phys. Rev. B **100**, 201406 (2019).
[22] S. Mittal, V. V. Orre, G. Zhu, M. A. Gorlach, A. Poddubny, and M. Hafezi, Nat. Photonics **13**, 692 (2019).
[23] X. Ni, M. Weiner, A. Alù, and A. B. Khanikaev, Nat. Mater. **18**, 113 (2019).
[24] X. Ni, M. Li, M. Weiner, A. Alù, and A. B. Khanikaev, Nat. Commun. **11**, 2108 (2020).
[25] H. Xue, Y. Yang, F. Gao, Y. Chong, and B. Zhang, Nat. Mater. **18**, 108 (2019).

[26] A. Dutt, M. Minkov, I. A. D. Williamson, and S. Fan, Light Sci. Appl. **9**, 131 (2020).
[27] B. Xie, H.-X. Wang, X. Zhang, P. Zhan, J.-H. Jiang, M. Lu, and Y. Chen, Nat. Rev. Phys. **3**, 520 (2021).
[28] W. Zhang, X. Xie, H. Hao, J. Dang, S. Xiao, S. Shi, H. Ni, Z. Niu, C. Wang, K. Jin, X. Zhang, and X. Xu, Light Sci. Appl. **10**, 167 (2021).
[29] M. Kim and J. Rho, Nanophotonics **9**, 3227 (2020).
[30] T. Fukui and Y. Hatsugai, Phys. Rev. B **98**, 035147 (2018).
[31] Q. Wang, D. Wang, and Q.-H. Wang, Europhys. Lett. **124**, 50005 (2018).
[32] H. Araki, T. Mizoguchi, and Y. Hatsugai, Phys. Rev. Research **2**, 012009 (2020).
[33] Y. You, J. Bibo, and F. Pollmann, Phys. Rev. Research **2**, 033192 (2020).
[34] Y. You, T. Devakul, F. J. Burnell, and T. Neupert, Phys. Rev. B **98**, 235102 (2018).
[35] O. Dubinkin and T. L. Hughes, Phys. Rev. B **99**, 235132 (2019).
[36] A. Rasmussen and Y.-M. Lu, Phys. Rev. B **101**, 085137 (2020).
[37] J. Guo, J. Sun, X. Zhu, C.-A. Li, H. Guo, and S. Feng, J. Phys. Condens. Matter **34**, 035603 (2022).
[38] J. Bibo, I. Lovas, Y. You, F. Grusdt, and F. Pollmann, Phys. Rev. B **102**, 041126 (2020).
[39] M. Lohse, C. Schweizer, O. Zilberberg, M. Aidelsburger, and I. Bloch, Nat. Phys. **12**, 350 (2016).
[40] M. Lohse, C. Schweizer, H. M. Price, O. Zilberberg, and I. Bloch, Nature (London) **553**, 55 (2018).
[41] H.-I. Lu, M. Schemmer, L. Aycock, D. Genkina, S. Sugawa, and I. Spielman, Phys. Rev. Lett. **116**, 200402 (2016).
[42] S. Nakajima, T. Tomita, S. Taie, T. Ichinose, H. Ozawa, L. Wang, M. Troyer, and Y. Takahashi, Nat. Phys. **12**, 296 (2016).
[43] F. Grusdt, M. Höning, and M. Fleischhauer, Phys. Rev. Lett. **110**, 260405 (2013).
[44] M. Aidelsburger, M. Atala, S. Nascimbène, S. Trotzky, Y.-A. Chen, and I. Bloch, Phys. Rev. Lett. **107**, 255301 (2011).
[45] S. Nascimbène, Y.-A. Chen, M. Atala, M. Aidelsburger, S. Trotzky, B. Paredes, and I. Bloch, Phys. Rev. Lett. **108**, 205301 (2012).
[46] M. Aidelsburger, M. Atala, M. Lohse, J. T. Barreiro, B. Paredes, and I. Bloch, Phys. Rev. Lett. **111**, 185301 (2013).
[47] H.-N. Dai, B. Yang, A. Reingruber, H. Sun, X.-F. Xu, Y.-A. Chen, Z.-S. Yuan, and J.-W. Pan, Nat. Phys. **13**, 1195 (2017).
[48] D. J. Thouless, M. Kohmoto, M. P. Nightingale, and M. den Nijs, Phys. Rev. Lett. **49**, 405 (1982).
[49] See Supplemental Material at http://link.aps.org/supplemental/10.1103/PhysRevLett.128.246602 for detailed proofs and more information on the generalization of Resta's argument. It includes Refs. [50–52].
[50] G. Ortiz and R. M. Martin, Phys. Rev. B **49**, 14202 (1994).
[51] T. Kato, J. Phys. Soc. Jpn. **5**, 435 (1950).
[52] R. Resta and D. Vanderbilt, *Physics of Ferroelectrics: A Modern Perspective* (2007), p. 31.
[53] M. V. Berry, Proc. R. Soc. A **392**, 45 (1984).